GEOPHYSICS, VOL. 67, NO. 5 (SEPTEMBER-OCTOBER 2002); P. 1406–1414, 5 FIGS., 1 TABLE.
10.1190/1.1512786

An approximation for the Xu-White velocity model

Robert G. Keys* and Shiyu Xu*

ABSTRACT

In 1995, S. Xu and R. E. White described a method for estimating compressional and shear-wave velocities of shaley sandstones from porosity and shale content. Their model was able to predict the effect of increasing clay content on compressional-wave velocity observed in laboratory measurements. A key step in the Xu-White method estimates dry rock bulk and shear moduli for the sand/shale mixture. This step is performed numerically by applying the differential effective medium method to the Kuster-Toksöz equations for ellipsoidal pores. This step is computationally intensive. Using reasonable assumptions about dry rock elastic properties, this step can be replaced with a set of approximations for dry rock bulk and shear moduli. Numerical experiments show an extremely close match between velocities obtained with these approximations and velocities computed with the differential effective medium method. These approximations simplify the application of the Xu-White method, and make the method computationally more efficient. They also provide insight into the Xu-White method. For example, these approximations show how the Xu-White model is related to the critical porosity model.

INTRODUCTION

Experimental data (e.g., Han et al., 1986) show that sonic velocities of sandstone are sensitive to porosity and clay content. Xu and White (1995) developed a method for predicting sonic velocities that accounts for the effects of these two important rock properties. Their model was able to predict the effect of increasing clay content on compressional-wave velocity observed in laboratory measurements by Marion et al. (1992). The Xu-White model attributes the effect of clay content on sonic velocity to pore geometry or pore aspect ratio differences between shale and sandstone pores. Aspect ratio refers to the ratio between the minor and major axes of an ellipsoidal pore. Since shales are composed of sheetlike particles, shale pores have much smaller aspect ratios than sandstone pores. Shale pores with small aspect ratios are more compliant than sandstone pores with larger aspect ratios, and thus pore geometry can have a significant effect on sonic velocity.

To account for the effect of pore geometry, Xu and White (1995) divide the pore space into compliant shale pores with small aspect ratios and stiff sandstone pores with large aspect ratios. If ϕ denotes porosity, then

$$\phi = \phi_S + \phi_C \tag{1}$$

where ϕ_S is the portion of the rock occupied by stiff or sandstone pores, and ϕ_C is the porosity associated with compliant or shale pores. The fractional volume of clay comprising the rock matrix, v_C, and sand volume fraction v_S are used to estimate ϕ_C and ϕ_S. Since $v_C + v_S = 1$, assuming that ϕ_C and ϕ_S are proportional to v_C and v_S, respectively, implies that

$$\phi_C = v_C\phi \tag{2}$$

and

$$\phi_S = v_S\phi. \tag{3}$$

Having divided the pore space into compliant and stiff pores, Xu and White determine the elastic properties of the dry frame using the Kuster and Toksöz (1974) equations for bulk and shear modulus:

$$K_d - K_m = \frac{1}{3}(K' - K_m)\frac{3K_d + 4\mu_m}{3K_m + 4\mu_m}\sum_{l=S,C}\phi_l T_{iijj}(\alpha_l) \tag{4}$$

and

$$\mu_d - \mu_m = \frac{(\mu' - \mu_m)}{5}\frac{6\mu_d(K_m + 2\mu_m) + \mu_m(9K_m + 8\mu_m)}{5\mu_m(3K_m + 4\mu_m)} \times \sum_{l=S,C}\phi_l F(\alpha_l), \tag{5}$$

Presented at the 70th Annual International Meeting, Society of Exploration Geophysicists. Manuscript received by the Editor November 20, 2000; revised manuscript received March 28, 2002.
*Exxon Mobil Upstream Research Company, 3316 Richmond Ave., Houston, Texas 77252-2189. E-mail: r_g_keys@email.mobil.com; shiyu-xu@email.mobil.com.

where

$$F(\alpha) = T_{ijij}(\alpha) - \frac{T_{iijj}(\alpha)}{3}. \quad (6)$$

In the Kuster-Toksöz equations (4) and (5), K_d, K_m, and K' are the bulk moduli of the dry frame, the rock matrix, and the pore inclusion material, respectively, and μ_d, μ_m, and μ' are the corresponding shear moduli. For dry rock, K' and μ' are zero. Also, α_S and α_C are the aspect ratios for the stiff and compliant pores; $T_{iijj}(\alpha)$ and $F(\alpha)$ are pore aspect ratio functions derived from the tensor T_{ijkl} that relates the uniform strain field at infinity to the strain field within an elastic ellipsoidal inclusion (Wu, 1966). The equations for the pore aspect ratio functions $T_{iijj}(\alpha)$ and $F(\alpha)$ are given in Appendix A.

The Kuster-Toksöz equations require $\phi/\alpha \ll 1$. Typical values for aspect ratios are 0.035 for shale pores and 0.12 for sandstone pores. Therefore, the Kuster-Toksöz equations are applicable only for very low porosity. To overcome this restriction, Xu and White (1995) use the differential effective medium method (Berryman, 1992) to incrementally increase the porosity of the rock.

To apply the differential effective medium method, the pore space is partitioned into sets of pores so that the pore concentration for each set satisfies the Kuster-Toksöz (1974) condition. Beginning with solid rock, the Kuster-Toksöz equations are used to compute the effective medium that results from adding a small set of pores to the matrix. The process is repeated, using the effective medium from the previous calculation as the rock matrix for the next calculation, until the total pore volume has been added to the rock. Xu and White (1995) used the Wyllie (1956) time average equations to estimate the solid rock bulk modulus K_0 and shear modulus μ_0 needed to start the process. However, other methods can be used to estimate the initial rock matrix moduli. This procedure yields the dry rock bulk and shear modulus of a rock with the specified porosity and pore aspect ratio.

Given the dry rock elastic moduli, Xu and White (1995) use Gassmann's equations (White, 1983, 60) to calculate the fluid saturated bulk and shear modulus, from which compressional and shear-wave velocity can be found:

$$K = K_d + \frac{\left(1 - \frac{K_d}{K_0}\right)^2}{\frac{\phi}{K_f} + \frac{(1-\phi)}{K_0} - \frac{K_d}{K_0^2}}, \quad (7)$$

$$\mu = \mu_d, \quad (8)$$

$$\rho = \phi\rho_f + (1-\phi)\rho_0, \quad (9)$$

$$V_P = \sqrt{\frac{\left(K + \frac{4}{3}\mu\right)}{\rho}}, \quad (10)$$

and

$$V_S = \sqrt{\frac{\mu}{\rho}}. \quad (11)$$

In equations (7)–(11), K is the bulk modulus of the fluid saturated rock, K_f is the bulk modulus of the pore fluid, and μ denotes the shear modulus of the fluid-saturated rock. Also, ρ_0 is the density of the rock matrix, ρ_f is the fluid density, and ρ is the density of the fluid saturated rock. Finally, V_P and V_S are the compressional- and shear-wave velocities of the fluid-saturated rock.

With this procedure, Xu and White (1995) were able to accurately predict compressional- and shear-wave velocities of shaley sands. The method accounts for the effects of fluids, porosity, and pore geometry on the elastic properties of a rock. However, the one drawback of the procedure is that the pore space must be partitioned into "sufficiently small" increments. How small is sufficiently small? Berryman (1992) and others addressed this issue by considering the consequences of allowing the incremental pore space to become vanishingly small.

THE DRY ROCK APPROXIMATION

Berryman (1992) showed that the equations for the differential effective medium technique converge to ordinary differential equations when the incremental porosity approaches zero. Let $K(\phi)$ denote the effective bulk modulus for porosity ϕ, and let $K(\phi + d\phi)$ be the effective bulk modulus obtained by adding the incremental porosity $d\phi/(1-\phi)$. Incremental porosity is normalized by $1-\phi$ because only the solid matrix component of the rock is replaced by pore space at each iteration. For the porosity ϕ, $K(\phi)$ can be regarded as the effective rock matrix bulk modulus and $K(\phi + d\phi)$ is the effective dry rock bulk modulus. Then $K(\phi)$ replaces K_m, the rock matrix bulk modulus, and $K(\phi + d\phi)$ replaces the dry rock bulk modulus K_d in the Kuster-Toksöz equation (4). Similarly, in equation (5), μ_m and μ_d are replaced by $\mu(\phi)$ and $\mu(\phi + d\phi)$, which denote the effective shear moduli for porosities ϕ and $\phi + d\phi$, respectively. If $d\phi$ is allowed to go to zero, then the Kuster-Toksöz equations (4) and (5) converge to

$$(1-\phi)\frac{dK}{d\phi} = \frac{1}{3}(K' - K)\sum_{l=S,C} v_l T_{iijj}(\alpha_l), \quad (12)$$

$$(1-\phi)\frac{d\mu}{d\phi} = \frac{1}{5}(\mu' - \mu)\sum_{l=S,C} v_l F(\alpha_l). \quad (13)$$

In equations (12) and (13), v_S and v_C are the sand and clay fractional volumes of the rock matrix associated with stiff and compliant pores, respectively.

These equations seem simpler than the Kuster-Toksöz equations (4) and (5), but actually they are as difficult to solve because the factors T_{iijj} and F depend on K, μ, and ϕ. Equations (12) and (13) are coupled nonlinear ordinary differential equations. Their solution must be computed numerically with a procedure similar to the iterative process described in the previous section. Some significant simplifications are possible for the case of dry rock, however.

For dry rock, $K' = \mu' = 0$. From Appendix A, T_{iijj} and F depend on K, μ, and ϕ through the scalars

$$A = \frac{\mu'}{\mu} - 1, \quad B = \frac{1}{3}\left(\frac{K'}{K} - \frac{\mu'}{\mu}\right), \text{ and } R = \frac{3\mu}{3K + 4\mu}.$$

Since $K' = \mu' = 0$, then $A = -1$ and $B = 0$.

Also, dry rock Poisson's ratio is often observed to be approximately constant with respect to porosity (Pickett, 1963; Krief et al., 1990; Brie et al., 1995). For an isotropic elastic solid, $R = (1-2\sigma)/(2-2\sigma)$, where σ is Poisson's ratio. If the dry rock Poisson's ratio σ is constant, then so is R. Consequently, both T_{iijj} and F are approximately constant with respect to ϕ.

Define a set of "coefficients" p and q and assume that σ is constant:

$$p = \frac{1}{3}\sum_{l=S,C} v_l T_{iijj}(\alpha_l) \tag{14}$$

and

$$q = \frac{1}{5}\sum_{l=S,C} v_l F(\alpha_l). \tag{15}$$

Then for dry rock, equation (12) becomes $(1-\phi)(dK/d\phi)+Kp=0$. Multiplying both sides of this equation by $(1-\phi)^{-p-1}$ shows that

$$(1-\phi)^{-p}\frac{dK}{d\phi} + Kp(1-\phi)^{-p-1} = 0. \tag{16}$$

Since p is constant, $(d/d\phi)[(1-\phi)^{-p}K] = (1-\phi)^{-p}(dK/d\phi)+Kp(1-\phi)^{-p-1}$, and from equation (16) it follows that $(1-\phi)^{-p}K(\phi)$ is constant with respect to ϕ. Therefore, $(1-\phi)^{-p}K(\phi) = K(0)$. Since $K(0)$ is the rock matrix bulk modulus K_0, then

$$K(\phi) = K_0(1-\phi)^p. \tag{17}$$

$K(\phi)$ is the dry rock bulk modulus for porosity ϕ. A similar argument shows that

$$\mu(\phi) = \mu_0(1-\phi)^q, \tag{18}$$

where μ_0 is the rock matrix shear modulus and $\mu(\phi)$ is the dry rock shear modulus for porosity ϕ. We refer to equations (17) and (18) as the "dry rock approximation" because they approximate the dry rock bulk and shear modulus calculated from the differential effective medium method.

The Xu-White method can be implemented with the dry rock approximation instead of repeatedly solving the Kuster-Toksöz (1974) equations (4) and (5) with incrementally increasing porosities to estimate the dry rock elastic moduli. This procedure is far easier to apply than the conventional Xu-White method, but how well does it work?

To test the dry rock approximation, we computed compressional and shear-wave velocities for brine-saturated rocks with different porosities and pore aspect ratios using both the dry rock approximation and the conventional Xu-White method. For this experiment, we assumed the rock matrix has a compressional-wave velocity of 5850 m/s, shear-wave velocity is 3900 m/s, and rock matrix density is 2.65 gm/cm^3. We also assumed that the fluid velocity is 1600 m/s, and fluid density is 1.1 gm/cm^3. These values are consistent with a quartz rock matrix and brine pore fluid, and match the values used by Xu and White (1995) to test their velocity model.

First, we computed the rock matrix bulk and shear moduli from the rock matrix properties. Next, using both the differential effective medium method and the dry rock approximation, we calculated the dry rock bulk and shear moduli for different pore aspect ratios (0.01, 0.05, 0.10, and 0.15) and for porosities from 0 to 0.4. For this experiment, stiff and compliant pore aspect ratios are equal. Finally, we used Gassmann's equations to calculate the brine-saturated elastic properties, including compressional and shear-wave velocity. The results of this experiment are shown in Figure 1. The maximum difference between compressional-wave velocity predicted with

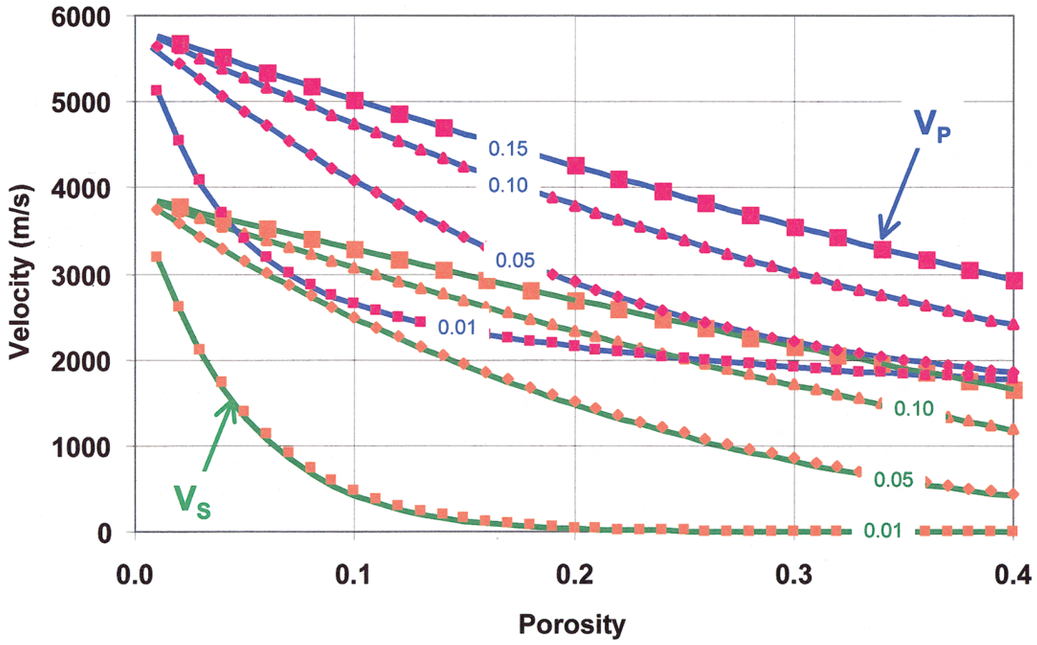

FIG. 1. Dry rock approximation versus conventional Xu-White method. Solid blue curves denote compressional-wave velocities computed with the conventional Xu-White method; red symbols show corresponding compressional-wave velocities calculated with the dry rock approximation. Solid green curves show shear-wave velocities obtained with the conventional Xu-White method for different pore-aspect ratios. Orange symbols show corresponding shear-wave velocities obtained with the dry rock approximation. Stiff and compliant pore aspect ratios were equal for this comparison. Pore aspect ratios are given as blue (compressional-wave velocity) and green (shear-wave velocity) numbers.

the dry rock approximation and compressional-wave velocity derived from the conventional Xu-White method is less than 0.7%. The percentage error is larger for shear-wave velocity, because the shear-wave velocity approaches zero for small aspect ratios. The maximum absolute error for shear-wave velocity is less than 60 m/s, which corresponds to a relative error of approximately 6%.

Figure 1 shows that the difference between the dry rock approximation and the conventional Xu-White method is very small. We found that the accuracy of the dry rock approximation decreases as dry rock Poisson's ratio increases. However, for typical values of dry rock Poisson's ratio (less than 0.25; Dvorkin et al., 1999), the dry rock approximation can be used in place of the differential effective medium method to calculate elastic moduli for the Xu-White method without affecting the final result.

Note that the equations (17) and (18) for bulk and shear modulus imply that dry rock Poisson's ratio is constant if and only if $p = q$. For sandstonelike aspect ratios near 0.2, p and q are almost equal but, in general, the dry rock Poisson's ratio obtained from equation (17) and (18) is not constant.

The reason the dry rock approximation can yield a porosity-dependent dry rock Poisson's ratio is because the constant Poisson's ratio condition applies only to the coefficients p and q. In Appendix B, we show that the error of the dry rock approximation is bounded by the variation in p and q with respect to porosity. The constant Poisson's ratio condition is a good assumption for calculating p and q, but it is not a good assumption for the actual predicted dry rock Poisson's ratio since some variation with porosity is necessary to accurately predict compressional and shear-wave velocities for sand/shale mixtures.

Since the dry rock approximation does not require the iterative solution of a system of equations, its use provides significant computational savings. The dry rock approximation also provides insight into properties of the Xu-White method.

PROPERTIES OF THE DRY ROCK APPROXIMATION

The dry rock approximation has some theoretical implications for the Xu-White model. For example, the differential effective medium method is known to be sensitive to the order in which pores are added to the host rock. Interchanging the host material with the inclusion material can give very different results for the elastic properties of the rock. This raises a concern for the Xu-White method about the order in which compliant and stiff pores are added to rock. Will a different answer result if compliant pores are added to the rock before the stiff pores rather than the other way around? Experience with the Xu-White method suggests that this is not a problem. The dry rock approximation explains why.

Let $p_C = (1/3)v_C T_{iijj}(\alpha_C)$ and $p_S = (1/3)v_S T_{iijj}(\alpha_S)$. Then from equation (14), $p = p_C + p_S$. From the dry rock approximation, the bulk modulus for stiff pores is $K_S = K_0(1-\phi)^{p_S}$. Compliant pores are added by multiplying the stiff pore bulk modulus by $(1-\phi)^{p_C}$. The resulting bulk modulus is

$$K_S(1-\phi)^{p_C} = K_0(1-\phi)^{p_S+p_C} = K_0(1-\phi)^{p}. \quad (19)$$

On the other hand, the compliant pore bulk modulus is $K_C = K_0(1-\phi)^{p_C}$. Adding the stiff pores is accomplished by multiplying by $(1-\phi)^{p_S}$. In this case, the bulk modulus is

$$K_C(1-\phi)^{p_S} = K_0(1-\phi)^{p_C+p_S} = K_0(1-\phi)^{p}. \quad (20)$$

The right-hand side of equations (19) and (20) match, which shows that the order in which pores are added has no effect on the final elastic moduli. Similar arguments show that the dry rock approximation for shear modulus is also independent of the order in which pores are added. These conclusions apply to the Xu-White method to the extent that the dry rock approximation holds.

The dry rock approximation also yields insight into the relation between the Xu-White model and other rock physics models. The critical porosity model (Nur et al., 1995) is a popular model that assumes dry rock bulk modulus varies linearly with respect to porosity for porosities less than some critical porosity. For porosities greater than the critical porosity, the rock behaves as a suspension and its bulk modulus is given by the Reuss average of the fluid and mineral bulk moduli. For porosities less than the critical porosity, the rock is said to be in the load-bearing domain and behaves as a solid material. Most geophysical applications of the critical porosity model are concerned with porosities in the load-bearing domain. The dry rock approximation relates the Xu-White method to the critical porosity model in the load-bearing domain where porosity is less than critical porosity.

For sufficiently small ϕ, $K_0(1-\phi)^p \approx K_0(1-p\phi)$, where p is given by equation (14). Defining

$$\phi_{crit} = 1/p, \quad (21)$$

then

$$K(\phi) = K_0(1-\phi/\phi_{crit}). \quad (22)$$

Equation (22) is the critical porosity model for dry rock bulk modulus in the load-bearing domain when $\phi < \phi_{crit}$. Since $\phi_{crit} = 1/p$, critical porosity can be related to pore aspect ratio. Figure 2 shows critical porosity as a function of pore aspect ratio, calculated from equations (14) and (21). Aspect ratios of stiff and compliant pores were assumed to be equal for this calculation. Figure 2 indicates that critical porosity increases with increasing pore aspect ratio.

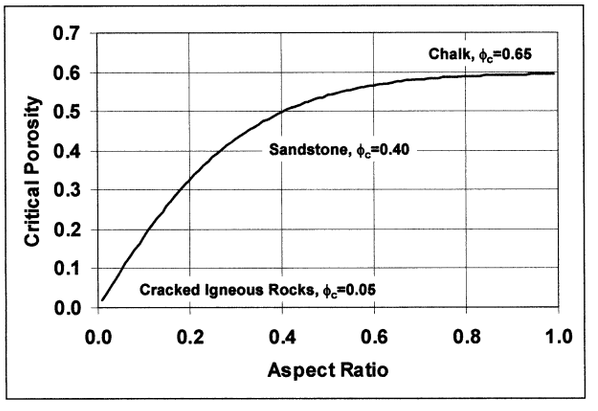

FIG. 2. Relationship between critical porosity and pore aspect ratio. Critical porosity increases with increasing pore aspect ratio. Predicted critical porosities are qualitatively consistent with measured critical porosities for several rock types.

Critical porosities have been published for several rock types (Mavko et al, 1996, 243). Although corresponding pore aspect ratios are not given, these data qualitatively support the predicted critical porosity curve shown in Figure 2. Cracked igneous rocks, such as fractured granites, are reported to have a critical porosity of 0.05. We expect fractures to have a small aspect ratio, and Figure 2 predicts that cracked igneous rocks should have pore aspect ratios of approximately 0.03. Sandstone has a critical porosity of 0.40. Sandstone should have a larger pore aspect ratio than fractured igneous rock, and Figure 2 predicts that the pore aspect ratio for sandstone is 0.27. Chalks have a critical porosity of 0.65, and Figure 2 suggests that chalks should have a large pore-aspect ratio, greater than 0.7. Thus, these measured data are qualitatively consistent with the predicted critical porosity curve shown in Figure 2.

Equations (21) and (22) show that the critical porosity model can be thought of as a first-order approximation to the dry rock approximation. In this context, the dry rock approximation yields additional insight into the critical porosity model. A rock is said to be in a state of suspension if pore fluid pressure supports the rock when a seismic wave passes through it. Pore fluid tends to dominate the support mechanism for rocks with small aspect-ratio pores, since small aspect-ratio pores, (e.g., microcracks), are very compliant. Rocks of this type, such as cracked igneous rocks, tend to be in a state of "suspension." This state of suspension is actually a pseudosuspension or suspension-like state since pore stiffness is not zero. A true suspension exists only when pore stiffness is zero.

On the other hand, large aspect-ratio pores, such as those found in chalks or volcanic rocks, are very stiff. In these rocks, the frame tends to bear most of the load for a passing seismic wave. Rocks with large aspect-ratio pores are unlikely to be in a state of suspension until porosity is very high. Of course, real rocks are far more complicated because pore stiffness also changes with porosity.

To be useful, the dry rock approximation must be an effective replacement for the conventional Xu-White method in applications for which the Xu-White method is commonly used. One of the uses for the Xu-White method is porosity estimation. In the next section, we use the dry rock approximation to estimate porosity from a sonic log. This procedure can also be used to predict shear-wave velocity from a compressional-wave sonic log and a shale volume curve.

AN APPLICATION FOR THE DRY ROCK APPROXIMATION

Figure 3 shows a set of log data from well A of the Mobil AVO Data Set (Keys and Foster, 1998). In Figure 3c, it is evident that porosity exceeds the theoretical maximum of about 40% at a number of points. The caliper log (Figure 3d) shows that many of the questionable porosity values correlate with borehole washouts. Since the sonic log is usually less sensitive to borehole washouts, it is sometimes used to estimate porosity. In this exercise, we use the dry rock approximation to the Xu-White method to estimate porosity from the compressional-wave sonic log and compare the results to the conventional Xu-White method.

Since the Xu-White method predicts compressional-wave velocity from shale content and porosity, it can be used in an inversion mode to estimate a porosity curve that matches the measured compressional-wave velocity. From the gamma-ray log in Figure 3b, we estimated shale volume over the depth

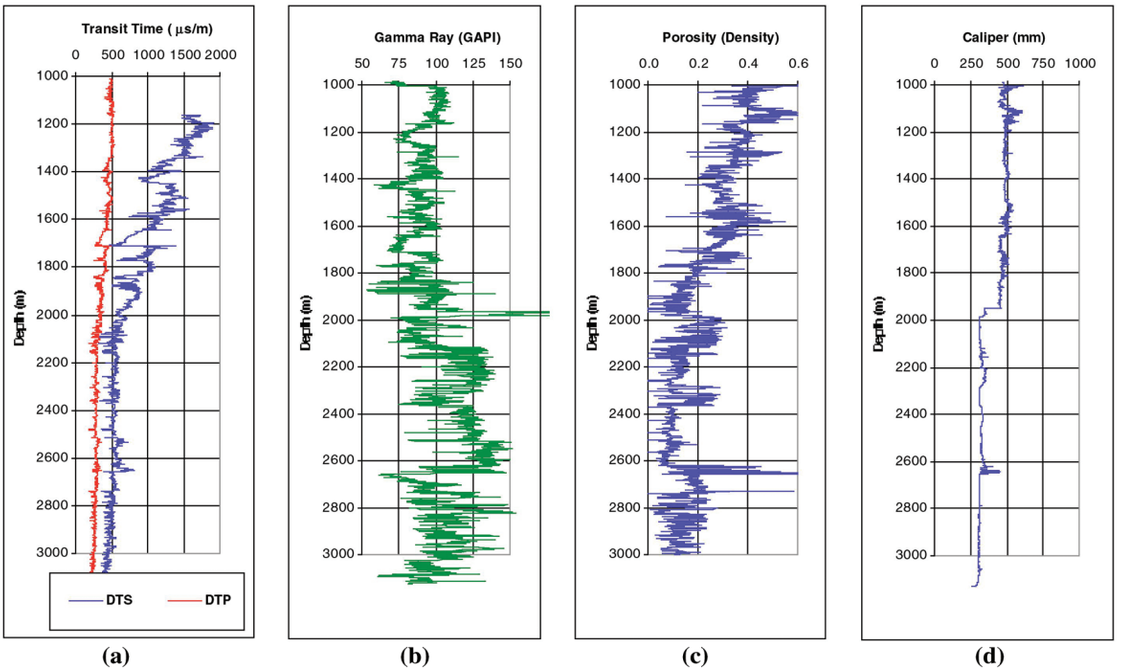

FIG. 3. Log data from well A, Mobil AVO Data Set. (a) DTP, compressional-wave sonic (red), and DTS, shear-wave sonic (blue); (b) gamma-ray log; (c) porosity curve estimated from density log; (d) caliper log. Estimated porosities exceed 40% at some depths, corresponding to washouts.

interval from 1000 to 3000 m. We used the Voigt-Reuss-Hill average based on the shale volume curve to calculate the rock matrix elastic moduli based on the elastic properties for sand and clay listed in Table 1. We derived fluid density and fluid bulk-modulus curves from the fluid properties and oil, gas, and brine saturation curves provided with the Mobil AVO data set. Finally, we assumed the nominal values for the pore aspect ratios listed in Table 1, and we set the dry rock Poisson's ratio to be 0.10. Using the shale volume curve derived from the gamma-ray log, we calculated a porosity curve to match the measured compressional-wave sonic over the depth interval from 1000 to 3000 m. The results are shown in Figure 4.

Figure 4a compares the predicted and measured compressional-wave sonic curves. Since porosity was determined to match the measured compressional-wave transit time, it is not surprising that these curves overlay one another. Figure 4b shows the predicted and measured shear-wave sonic curves. No constraint was imposed on the predicted shear-wave transit time, so the extent to which the predicted and measured shear-wave sonic match is a measure of the reliability of the porosity estimation. Figure 4c compares the porosity estimated from the density log to the porosity derived using the dry rock approximation to the Xu-White method. The two porosity curves match over intervals where the caliper log indicates the borehole is in good condition. Major differences between the porosity curves occur where the caliper indicates borehole washouts. At these locations, the density-estimated porosity exceeds theoretical limits, but the Xu-White porosity estimate remains within theoretical limits over the entire depth interval of the log.

The match between the predicted and measured shear-wave logs and the correspondence between the two porosity curves over intervals where the borehole is in good condition support the accuracy of the porosity estimate from the dry rock approximation. At the very least, these results show that the dry rock porosity estimate is consistent with the observed log data.

The main objective of this test is to compare the conventional Xu-White method to the dry rock approximation. Figure 5 shows the compressional and shear-wave transit times calculated with the conventional Xu-White method using the sonic-log porosity curve in Figure 4. Figure 5a shows the compressional-wave transit time derived from the dry rock approximation (blue) and the compressional-wave transit time derived from the conventional Xu-White method (red) using the differential effective medium method (DEM). The curves overlay, indicating that for porosity estimation, the two

Table 1. Rock properties for porosity estimation, well A.

Rock Type	Compressional-wave Transit Time (μs/m)	Shear-wave Transit Time (μs/m)	Density (gm/cm^3)	Pore Aspect Ratio
Sand	166	256	2.65	0.10
Clay	230	394	2.65	0.04

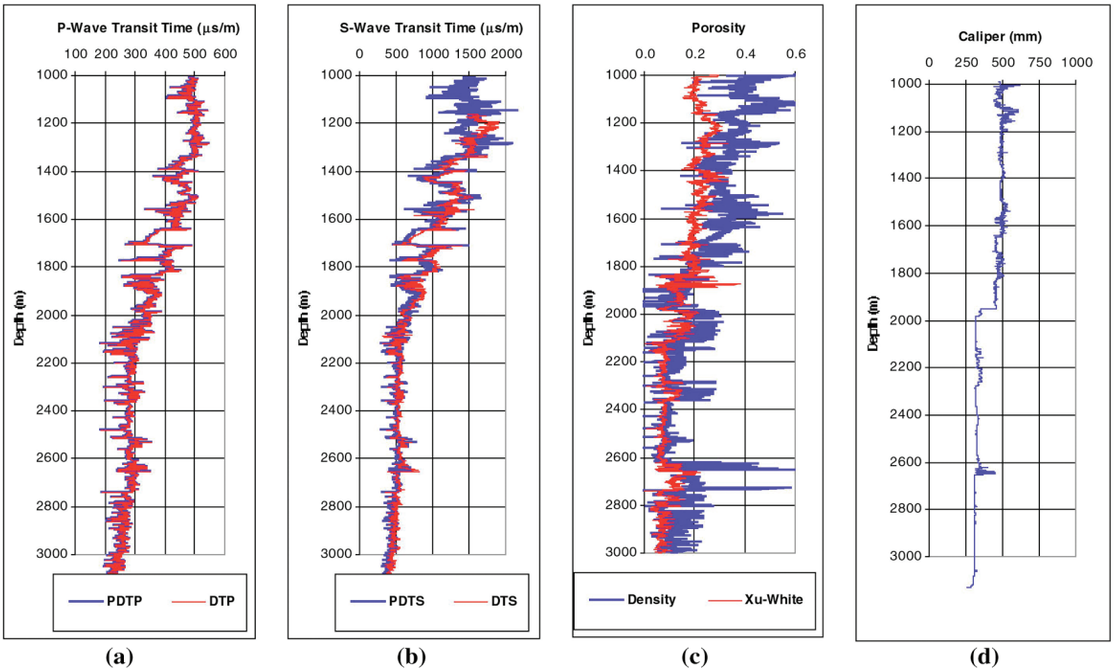

FIG. 4. Porosity estimation for well A, Mobil AVO Data Set. (a) PDTP, predicted (blue) versus DTP, measured (red) compressional-wave sonic log; (b) PDTS, predicted (blue) versus DTS, measured (red) shear-wave sonic log; (c) porosity derived from density log (blue) versus porosity derived from Xu-White method (red); (d) caliper log. Match between predicted and measured shear-wave sonic curves are an indication of the reliability of the porosity derived from the Xu-White method. Xu-White predicted porosity falls within theoretical limits for sandstone porosity.

procedures yield indistinguishable results. In Figure 5c, the percent difference in compressional-wave transit time is much less than 1%, and the difference in shear-wave transit times is approximately 2% over most of the depth interval. The larger shear-wave transit time above 1800 m is responsible for the smaller relative error in this interval. Absolute error in shear-wave transit time decreases with depth as shear-wave velocity increases.

Although the two methods yield almost identical results, there is a large difference in computation time. In this test, use of the dry rock approximation improved computation time by a factor of 50. This time savings can be significant in inversion applications like porosity estimation that require multiple evaluations of the Xu-White model.

CONCLUSIONS AND DISCUSSION

By assuming dry rock Poisson's ratio is constant in equations (14) and (15) for the coefficients p and q, the differential effective medium equations for dry rock bulk and shear modulus have an analytic solution: the dry rock approximation. As shown in Appendix B, the accuracy of the dry rock approximation depends on the variation with respect to porosity of p and q, which is small when dry rock Poisson's ratio is constant.

Although a constant dry-rock Poisson's ratio was assumed for the calculation of p and q, the Poisson's ratio derived from the dry rock approximation is not constant, in general, because the constant dry-rock Poisson's ratio assumption applies only to the p and q coefficients. This condition is less restrictive than other methods that force dry rock Poisson's ratio to be constant. Moreover, it is desirable that dry rock Poisson's ratio is allowed to vary since a constant dry-rock Poisson's ratio yields a poor approximation for shear-wave velocity.

Accuracy of the dry rock approximation degrades as dry rock Poisson's ratio increases, but for dry rock Poisson's ratios less than 0.25; the dry rock approximation has sufficient accuracy to replace the DEM calculations for typical applications of the Xu-White method.

For many methods, there is often a concern about fluid substitution in shaley sands. The key issue is the treatment of the microporosity associated with the compliant shale pores. Traditionally, it is expected that microporosity is always water-wet. One approach to this issue is to include microporosity in the rock matrix since the local permeability for micropores is so low that they are effectively isolated. However, we must then guess the elastic properties of the "rock matrix" which contains the microporosity. This is difficult because microporosity varies with pressure, temperature, and even the chemistry of the clay minerals.

The dry rock approximation can be adapted to handle the microporosity issue. Specifically, we use the compliant pore bulk modulus K_C [left-hand side of equation (20)] to add the micropores to the rock matrix. After substituting brine into the micropores, we then use the stiff component of equation (20) to add the stiff pores. We found that this two-step procedure (we add water-wet compliant pores separately from the stiff pores) provides a good match to laboratory data for a generalization of the dry rock approximation to the anisotropic case.

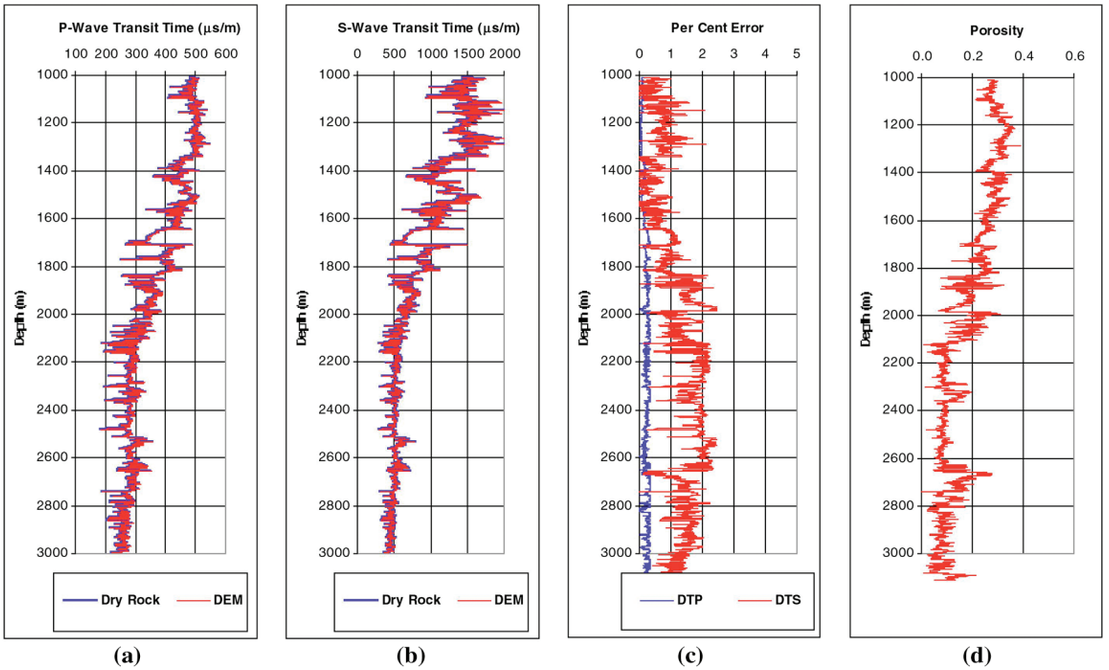

FIG. 5. Dry rock approximation versus conventional Xu-White method. Porosity curve (d) was computed with the dry rock approximation. This porosity curve was used to derive compressional and shear-wave transit times with the conventional Xu-White method (DEM). Maximum compressional-wave error is much less than 1%. Maximum Shear-wave error is less than 2%. (a) Compressional-wave transit time: dry rock approximation (blue) versus conventional Xu-White method (red); (b) shear-wave transit time: dry rock approximation (blue) versus conventional Xu-White method (red); (c) percent difference between dry rock approximation and conventional Xu-White method: DTP, compressional-wave transit time error (blue), DTS, shear-wave transit time error (red); (d) Porosity from dry rock approximation.

Used in place of the DEM method, the dry rock approximation yields transit times that closely match compressional- and shear-wave transit times computed with the conventional Xu-White method. The dry rock approximation significantly reduces the computational effort required to estimate transit times or velocities compared to the conventional Xu-White method. It also yields insight into the Xu-White method. It explains why the Xu-White method is insensitive to the order in which compliant or stiff pores are added to the rock matrix, and shows how the Xu-White method is related to other well-known rock physics models, such as the critical porosity model. With the dry rock approximation, critical porosity can be related to pore aspect ratio.

ACKNOWLEDGMENTS

The authors thank Wences Gouveia, Denis Schmitt, and the reviewers for comments and suggestions that improved this article. We also thank Exxon Mobil Upstream Research Company for allowing us to publish this work.

REFERENCES

Berryman, J. G., 1980, Long-wavelength propagation in composite elastic media II: Ellipsoidal inclusions: J. Acoust. Soc. Am., **68**, 1820–1831.

——— 1992, Single-scattering approximations for coefficients in Biot's equations of poroelasticity: J. Acoust. Soc. Am., **91**, 551–571.

Brie, A., Pampuri, F., Marsala, A. F., and Meazza, O., 1995, Shear sonic interpretation in gas-bearing sands: Ann. Tech. Conf., Soc. Petr. Eng., SPE 30595.

Dvorkin, J., Moos, D., Packwood, J. L., and Nur, A., 1999, Identifying patchy saturation from well logs: Geophysics, **64**, 1756–1759.

Han, D., Nur, A., and Morgan, D., 1986, Effect of porosity and clay content on wave velocity in sandstones: Geophysics, **51**, 2093–2107.

Keys, R. G., and Foster, D. J., 1998, Comparison of seismic inversion methods on a single real data set: Soc. Explor. Geophys. Open File Publications **4**.

Krief, M., Garat, J., Stellingwerff, J., and Ventre, J., 1990, A petrophysical interpretation using the velocities of P and S waves (full-waveform sonic): The Log Analyst, **31**, 355–369.

Kuster, G. T., and Toksöz, M. N., 1974, Velocity and attenuation of seismic waves in two-phase media: Part 1: Theoretical formulation: Geophysics, **39**, 587–606.

Marion, D., Nur, A., Yin, H., and Han, D., 1992, Compressional velocity and porosity in sand-clay mixtures: Geophysics, **57**, 554–563.

Mavko, G., Mukerji, T., and Dvorkin, J., 1996, Rock physics handbook: Stanford Rock Physics Laboratory.

Nur, A., Mavko, G., Dvorkin, J., and Gal, D., 1995, Critical porosity: The key to relating physical properties to porosity in rocks, 65th Ann. Internal. Mtg., Soc. Explor. Geophys., Expanded Abstracts 878.

Pickett, G. R., 1963, Acoustic character logs and their applications in formation evaluation: J. Petrol. Technol., **15**, 650–667.

White, J. E., 1983, Underground sound: Application of seismic waves: Elsevier Science Publishing Co. Inc.

Wu, T. T., 1966, The effect of inclusion shape on the elastic moduli of a two-phase material: Internat. J. Solids and Structures, **2**, 1–8.

Wyllie, M. R., Gregory, A. R., and Gardner, L. W., 1956, Elastic wave velocities in heterogeneous and porous media, Geophysics, **21**, 41–70.

Xu, S., and White, R. E., 1995, A new velocity model for clay-sand mixtures: Geophys. Prosp., **43**, 91–118.

APPENDIX A

PORE ASPECT RATIO FUNCTIONS

The pore aspect ratio functions $T_{iijj}(\alpha)$ and $F(\alpha)$ in the Kuster-Toksöz equations (4) and (5) are derived from a tensor T_{ijkl} that relates the uniform strain field at infinity to the strain field within an ellipsoidal elastic inclusion (Wu, 1966). The equations for $T_{iijj}(\alpha)$ and $F(\alpha)$ are given by Kuster and Toksöz (1974) and Xu and White (1995). Both papers contained some typographical errors, so the corrected formulas are repeated below. These formulas are mathematically equivalent to Berryman's (1980) formulas for oblate spheroids.

$$T_{iijj}(\alpha) = \frac{3F_1}{F_2} \tag{A-1}$$

and

$$F(\alpha) = \frac{2}{F_3} + \frac{1}{F_4} + \frac{F_4F_5 + F_6F_7 - F_8F_9}{F_2F_4}, \tag{A-2}$$

where

$$F_1 = 1 + A\left[\frac{3}{2}(g+\vartheta) - R\left(\frac{3}{2}g + \frac{5}{2}\vartheta - \frac{4}{3}\right)\right], \tag{A-3}$$

$$F_2 = 1 + A\left[1 + \frac{3}{2}(g+\vartheta) - \frac{R}{2}(3g+5\vartheta)\right] + B(3-4R) + \frac{A}{2}(A+3B)(3-4R)[g+\vartheta - R(g-\vartheta+2\vartheta^2)], \tag{A-4}$$

$$F_3 = 1 + \frac{A}{2}\left[R(2-\vartheta) + \frac{1+\alpha^2}{\alpha^2}g(R-1)\right], \tag{A-5}$$

$$F_4 = 1 + \frac{A}{4}[3\vartheta + g - R(g-\vartheta)], \tag{A-6}$$

$$F_5 = A\left[R\left(g+\vartheta-\frac{4}{3}\right) - g\right] + B\vartheta(3-4R), \tag{A-7}$$

$$F_6 = 1 + A[1 + g - R(\vartheta+g)] + B(1-\vartheta)(3-4R), \tag{A-8}$$

$$F_7 = 2 + \frac{A}{4}[9\vartheta + 3g - R(5\vartheta+3g)] + B\vartheta(3-4R), \tag{A-9}$$

$$F_8 = A\left[1 - 2R + \frac{g}{2}(R-1) + \frac{\vartheta}{2}(5R-3)\right] + B(1-\vartheta)(3-4R), \tag{A-10}$$

$$F_9 = A[g(R-1) - R\vartheta] + B\vartheta(3-4R), \tag{A-11}$$

$$A = \frac{\mu'}{\mu} - 1, \tag{A-12}$$

$$B = \frac{1}{3}\left(\frac{K'}{K} - \frac{\mu'}{\mu}\right), \tag{A-13}$$

$$R = \frac{3\mu}{3K + 4\mu} = \frac{1 - 2\sigma}{2 - 2\sigma}, \tag{A-14}$$

$$g = \frac{\alpha^2}{1 - \alpha^2}(3\vartheta - 2), \tag{A-15}$$

$$\vartheta = \frac{\alpha}{(1 - \alpha^2)^{3/2}}[\cos^{-1}(\alpha) - \alpha\sqrt{1 - \alpha^2}]. \tag{A-16}$$

In equations (A-12)–(A-14), K, and K' are the bulk moduli for the rock matrix and inclusion material, respectively; μ and μ' denote the shear moduli for the rock matrix and inclusion material, respectively; and σ is Poisson's ratio. In equations (A-15) and (A-16), α is the aspect ratio of the inclusion. For the dry rock approximation, K' and μ' are zero so that $A = -1$ and $B = 0$. Given the pore aspect ratio α and the dry rock Poisson's ratio σ, equations (A-1)–(A-16) determine the pore aspect ratio functions T_{iijj} and F.

APPENDIX B

ERROR BOUND FOR DRY ROCK APPROXIMATION

From equations (12) and (14), the differential equation for dry rock bulk modulus is

$$(1 - \phi)\frac{dK}{d\phi} = -pK, \tag{B-1}$$

with the initial condition

$$K(0) = K_0. \tag{B-2}$$

Since the coefficient p depends on porosity ϕ implicitly through Poisson's ratio, the solution of (B-1) and (B-2) can be written as

$$K(\phi) = K_0 \exp\left\{-\int_0^\phi \frac{p(\varphi)}{1 - \varphi}\, d\varphi\right\}. \tag{B-3}$$

Substituting equation (B-3) into equations (B-1) and (B-2) verifies that (B-3) is the solution of the differential equation and initial condition. From equation (17), the dry rock approximation $\hat{K}$ is

$$\hat{K}(\phi) = K_0(1 - \phi)^{\hat{p}}, \tag{B-4}$$

where $\hat{p}$ is the coefficient p evaluated for a fixed dry rock Poisson's ratio, usually the Poisson's ratio for the rock matrix. Using the identities

$$(1 - \phi)^{\hat{p}} = \exp\{\hat{p}\log(1 - \phi)\} \tag{B-5}$$

and

$$\log(1 - \phi) = -\int_0^\phi \frac{d\varphi}{1 - \varphi}, \tag{B-6}$$

the dry rock approximation (B-4) can be written as

$$\hat{K}(\phi) = K_0 \exp\left\{-\int_0^\phi \frac{\hat{p}}{1 - \varphi}\, d\varphi\right\}. \tag{B-7}$$

The absolute error for the dry rock approximation is

$$\varepsilon(\phi) = |K(\phi) - \hat{K}(\phi)|. \tag{B-8}$$

Inserting the dry rock bulk modulus (B-3) and the dry rock approximation (B-7) into the error formula (B-8) shows that the absolute error for the dry rock approximation is

$$\varepsilon(\phi) = K_0\left|\exp\left\{-\int_0^\phi \frac{p(\varphi)}{1 - \varphi}\, d\varphi\right\} - \exp\left\{-\int_0^\phi \frac{\hat{p}}{1 - \varphi}\, d\varphi\right\}\right|,$$

or

$$\varepsilon(\phi) = K(\phi)\left|1 - \exp\left\{\int_0^\phi \frac{p - \hat{p}}{1 - \varphi}\, d\varphi\right\}\right|. \tag{B-9}$$

Let $g(x) = |1 - \exp(x)| - |x|e^{|x|}$. The function $g(x)$ has a global maximum when x is zero. Thus, $g(x) \le g(0)$, from which it follows that

$$|1 - \exp(x)| \le |x|e^{|x|} \tag{B-10}$$

for all x. Applying the inequality (B-10) to the error formula (B-9) shows that

$$\varepsilon(\phi) \le K(\phi)\left|\int_0^\phi \frac{p - \hat{p}}{1 - \varphi} d\varphi\right| \exp\left\{\left|\int_0^\phi \frac{p - \hat{p}}{1 - \varphi} d\varphi\right|\right\}. \tag{B-11}$$

If $p(\varphi)$ is continuous for φ between 0 and ϕ, inclusive, then $\|p - \hat{p}\| = \max_{0 \le \varphi \le \phi} |p(\varphi) - \hat{p}|$ is finite and

$$\left|\int_0^\phi \frac{p(\varphi) - \hat{p}}{1 - \varphi}\, d\varphi\right| \le \|p - \hat{p}\| \int_0^\phi \frac{d\varphi}{1 - \varphi} = \|p - \hat{p}\||\log(1 - \phi)|. \tag{B-12}$$

From inequalities (B-11) and (B-12),

$$\varepsilon(\phi) \le K(\phi)\|p - \hat{p}\||\log(1 - \phi)| \times \exp\{-\|p - \hat{p}\|\log(1 - \phi)\}, \tag{B-13}$$

which simplifies to

$$\varepsilon(\phi) \le K(\phi)\|p - \hat{p}\||\log(1 - \phi)|(1 - \phi)^{-\|p - \hat{p}\|}. \tag{B-14}$$

The error bound (B-14) shows that the absolute error for the dry rock approximation goes to zero as porosity becomes small. More importantly, the error for the dry rock approximation depends on $\|p - \hat{p}\|$, which is small when the variation in dry rock Poisson's ratio is small. A similar error bound holds for the shear modulus.